NSM SHEAR STRENGTHENING TECHNIQUE WITH CFRP LAMINATES APPLIED IN HIGH T CROSS SECTION RC BEAMS

S. J. E. Dias[1] and J. A. O. Barros[2]

[1] Assistant Prof., ISISE, Dep. of Civil Eng., Univ. of Minho, Azurém, 4810-058 Guimarães, Portugal

[2] Full Prof., ISISE, Dep. of Civil Eng., Univ. of Minho, Azurém, 4810-058 Guimarães, Portugal

ABSTRACT

The effectiveness of the Near Surface Mounted (NSM) technique with Carbon Fiber Reinforced Polymer (CFRP) laminates for the shear strengthening of relatively high T cross section (h = 600 mm) Reinforced Concrete (RC) beams was assessed by experimental research. Two inclinations of the laminates were tested (52º and 90º) and, for each one, two percentages of CFRP were adopted. The RC beams shear strengthened with NSM laminates had a percentage of steel stirrups of 0.09%. The experimental results showed that NSM shear strengthening technique with CFRP laminates is very effective in RC beams of relatively high cross section height, not only in terms of increasing the load carrying capacity of the beams, but also in assuring higher mobilization of the tensile capacity of the CFRP. Furthemore, inclined laminates were more effective than vertical laminates and the shear capacity of the beams increased with the percentage of laminates. Taking into account available experimental results obtained with the same test setup, but using RC beams of lower depth of T cross section (h = 400 mm), it can be concluded that the effectiveness of the NSM technique with CFRP laminates increase with the increase of the depth of the cross section. The formulations provided by Nanni *et al.* (2004) and Dias and Barros (2013) for the NSM shear strengthening technique predicted a CFRP contribution around 51% and 67%, respectively, of the experimentally registered values.

KEYWORDS: NSM CFRP laminates; High T cross section RC beams; Shear strengthening; Experimental results; Analytical formulations.

1. INTRODUCTION

The shear failure mode of a reinforced concrete (RC) beam should be avoided because it is brittle and unpredictable. Due to high strength-to-weight ratio, high durability - non corrosive, electromagnetic neutrality, ease of handling, rapid execution with lower labor, and practically unlimited availability in size, geometry and dimension, carbon fiber reinforced polymer (CFRP) materials are being used as competitive alternatives on the structural rehabilitation of RC

---

[1] Author to whom the correspondence should be sent (sdias@civil.uminho.pt).

structures. For the shear strengthening, CFRP can be applied according to the followings two main techniques: Externally Bonded Reinforcement (EBR) where the CFRP (wet lay-up sheets or laminates) is bonded to the external faces of the elements to be strengthened, by full wrapping the cross section, or applying in a U configuration, or in the lateral faces of the beam [1-4]; Near Surface Mounted (NSM) where CFRP bars (circular, square or rectangular cross section) are introduced into pre-cut slits opened on the concrete cover of the elements to strengthen [5-8]. Due to the largest bond area and higher confinement provided by the surrounding concrete, narrow strips of CFRP laminates of rectangular cross section, installed into thin slits and bonded to concrete by an epoxy adhesive, are the most effective CFRP strengthening elements for the NSM technique [9].

Dias and Barros [10] concluded that NSM technique is more effective than EBR technique because NSM provided a larger increase of load carrying capacity after shear crack formation. The use of NSM technique better mobilized the tensile capacity of the CFRP reinforcement because higher tensile strains were measured in these composites when this technique was used. NSM requires no surface preparation work and, after cutting and cleaning the thin slits, the strengthening procedure is resumed to the installation of the CFRP laminates. A further advantage of the NSM technique is its ability to significantly reduce the probability of harm resulting from acts of vandalism, mechanical damages and aging effects. When NSM is used, the appearance of a structural element is practically unaffected by the strengthening intervention.

The effectiveness of NSM shear strengthening technique with CFRP laminates applied for T cross section RC beams with a certain percentage of steel stirrups was assessed by an extensive experimental research carried out by Dias and Barros [11]. In this context, the influence of the following parameters was appraised: concrete strength; percentage of existing steel stirrups; percentage and inclination of the CFRP laminates; existence of shear cracks when the RC beams are shear strengthened with NSM CFRP laminates. The tested RC beams with a T cross section of 400 mm height, had percentages of steel stirrups (ρ_{sw}) ranging between 0.10% and 0.17%. In terms of concrete strength, three types were basically used: low strength (f_{cm} = 18.6 MPa, where f_{cm} is the average concrete compressive strength at the age of the beams tests), medium strength (f_{cm} = 31.1 to 39.7 MPa), and high strength (f_{cm} = 59.4 MPa). Three orientations of the laminates with respect to the beam's axis were tested (θ_f = 90º - vertical laminates; θ_f = 45º - laminates at 45º; θ_f = 60º - laminates at 60º), and the levels of the CFRP percentage (ρ_f) analyzed ranged between 0.06% and 0.19%. Regardless of the percentage of CFRP, percentage of existing steel stirrups and concrete strength, inclined laminates were more effective than vertical laminates. It was also verified that the beam's shear capacity increased with ρ_f, while the NSM shear strengthening effectiveness decreased with the increase of the percentage of existing steel stirrups. The main difference of the behavior of NSM CFRP beams with and without pre-cracks resided in an expected loss of initial stiffness in the pre-cracked beams. However, the pre-cracking had not affected the efficacy of the NSM shear

strengthening technique in terms of load carrying capacity and ultimate deflection. The contribution of the NSM CFRP laminates for the beam shear resistance was limited by the concrete tensile strength. In fact, this technique was more effective when applied to RC beams of high-strength concrete, not only in terms of increasing the load carrying capacity of the beams, but also in assuring higher mobilization of the tensile capacity of the CFRP. This can be justified by the physical interpretation of the types of failure modes developed during the shear crack propagation bridged by NSM CFRP laminates described elsewhere [12]. However, considering the results of Dias and Barros [11], the shear strengthening can still be significant in RC beams of relatively low concrete strength if a convenient bond length for the CFRP laminates is assured.

There are several reasons that justify the relevance of a study on the use of the NSM technique with CFRP laminates for the shear strengthening of relatively high T cross section RC beams: these kind of beams is quite current in buildings and bridges; experimental results about the shear strengthening of RC beams using NSM technique with CFRP laminates indicate that the bond length of the CFRP has an important role in the effectiveness of this strengthening technique [11].

To appraise the possibility of the application of the NSM technique with CFRP laminates for the shear strengthening of relatively high T cross section RC beams having a certain percentage of existing steel stirrups, an experimental program was carried out. The height of the T cross section was 600 mm (h = 600 mm). The experimental program is outlined and the specimens, materials, test set-up and monitoring system are described. The results are presented and analyzed in terms of the structural behavior of the tested beams, modes of failure and effectiveness of the NSM CFRP shear strengthening configurations. Taking into account available experimental results obtained with the same test set-up but using RC beams of lower T cross section (h = 400 mm), the influence of the height of the RC beams in the performance of the NSM technique with CFRP laminates for the shear strengthening of RC beams was assessed.

Additionally, the predictive performance of the formulations proposed by Nanni *et al.* [13] and Dias and Barros [11] for the contribution of NSM CFRP systems for shear resistance of RC beams was appraised by taking the results obtained in the present experimental program.

2. EXPERIMENTAL PROGRAM

2.1 Beam prototypes

The experimental program was composed of five T cross section RC beams: a reference beam (Fig. 1) and four NSM CFRP shear strengthened beams (Fig. 2). The beams were 4600 mm long and the T cross section had overall dimensions of 450 mm (width of flange) by 600 mm (total depth). The width of the web and the thickness of the flange were 180 mm and 100 mm, respectively. Fig. 1 shows the T cross section geometry and the steel reinforcement details

for the series of beams, as well as the loading configuration and support conditions. The adopted reinforcement was designed to assure shear failure mode for all the tested beams. To localize the shear failure in only one of the beam shear spans, a three point loading configuration with a distinct length for the beam shear spans was selected, as shown in Fig. 1. The monitored beam span (*a*) was 2.5 times the effective depth of the beam (*a/d*=1400/558=2.5), since according to the available research [14], this is the minimum value that assures a negligible arch effect. To avoid shear failure in the *b* beam span, steel stirrups of 6 mm diameter at a spacing of 112 mm ($\phi6@112$ mm) were applied in this span. To prevent brittle spalling of the concrete cover at the supports, the beam's ends were strengthened by confining the concrete with a two-directional cage of $\phi6@65$ mm horizontal stirrups and $\phi10@50$ mm vertical stirrups (Fig. 1). To overcome the difficulties of bending the $\phi32$ mm longitudinal tensile bars, their ends were welded to a steel plate.

The differences between the tested beams were restricted to the CFRP shear reinforcement in the *a* beam span. The reference beam without CFRP was designated as "3S-R" (three steel stirrups in the *a* shear span leading a steel shear reinforcing ratio, ρ_{sw}, of 0.09%), while the following NSM strengthening configurations, with CFRP laminates of 1.4×10 mm^2 cross section, were adopted for the other four beams that also included three steel stirrups in the *a* shear span (Fig. 2 and Table 1): 3S-4LV beam with four CFRP laminates per face installed in vertical slits ($\theta_f = 90°$) with 350 mm of spacing; 3S-7LV beam with seven CFRP laminates per face installed in vertical slits ($\theta_f = 90°$) with 175 mm of spacing; 3S-4LI beam with four CFRP laminates per face with 350 mm of spacing and inclined at 52 degrees with respect to the longitudinal axis of the beam ($\theta_f = 52°$ - the same orientation of the line AB present in the beam 3S-4LI of the Fig. 2); 3S-9LI beam with nine CFRP laminates per face with 175 mm of spacing and inclined at 52 degrees with respect to the longitudinal axis of the beam ($\theta_f = 52°$).

The CFRP laminates were installed in slits executed from the bottom surface of the flange to the bottom tensile surface of the beam's web, i.e., bridging the total lateral surfaces of the beam's web (Fig. 3a). In fact, each CFRP laminate was installed in the outer part of a slit of a depth of 15 mm and a width of 5 mm executed on the beam's web lateral surfaces (the laminates were not anchored to the beam flange; they were restricted to the beam web). The configuration adopted for the CFRP laminates avoided any type of injury in the steel reinforcements during the execution of the slits (the concrete cover of the lateral faces of the beam's web was about 22 mm thickness). After opening the slits, the NSM strengthening technique is composed of the following procedures: 1) the slits were cleaned by compressed air; 2) the laminates were cleaned with acetone; 3) the epoxy adhesive was produced according to supplier recommendations; 4) the slits were filled with the adhesive; 5) the adhesive was applied on the faces of the laminates; and 6) the laminates were inserted into the slits (Fig. 3b) and adhesive in excess was removed. To guarantee a proper curing of the adhesive, at least one week passed between the beam strengthening operations and the beam test.

The details of the shear strengthening configurations are indicated in Table 1. This table shows that the tested beams had a percentage of longitudinal tensile steel bars (ρ_{sl}) of 2%, a percentage of steel stirrups (ρ_{sw}) of 0.09%, and a percentage of NSM CFRP laminates (ρ_f) ranging from 0.044% to 0.113%.

2.2 Material properties

The concrete compressive strength was evaluated when the beam tests were realized. In order to do it, direct compression tests were carried out with cylinders of 150 mm diameter and 300 mm hight, according to EN 206-1 [15]. At the age of the test of the 3S-R, 3S-4LV and 3S-4LI beams the value of f_{cm} (average compressive strength) was 36.4 MPa. At the age of the test of 3S-7LV and 3S-9LI beams the value of f_{cm} was 40.4 MPa. The values of the main tensile properties of the high bond steel bars used in the tested beams (Table 2) were obtained from uniaxial tensile tests performed according to the recommendations of EN 10002-1[16]. CFK 150/2000 S&P laminates were used in the present experimental research and the tensile properties were evaluated following the recommendations of ISO 527-5 [17]. The average value of the tensile strength (f_{fu}), elasticity modulus (E_f), and ultimate strain (ε_{fu}) of CFRP laminate was, respectively, 3009.3 MPa, 169.2 GPa and 17.8‰.

S&P Resin 220 epoxy adhesive was used to bond the CFRP laminates to the concrete substrate. The instantaneous and long term tensile behavior of this adhesive was investigated by Costa and Barros [18]. At 3 days, at which the elasticity modulus ($E_{0.5\sim2.5‰}$) attained a stabilized value, the tensile strength and the $E_{0.5\sim2.5‰}$ were determined in accordance with the ISO 527-2 recommendations [19], and the obtained results were 20 MPa and 7 GPa, respectively.

2.3 Test setup and monitoring system

Three point beam bending tests (Fig. 3c) were carried out using a servo closed-loop control equipment, taking the signal read in the displacement transducer (LVDT), placed at the loaded section, to control the test at a deflection rate of 0.01 mm/second. With the purpose to obtain the strain variation along two laminates that have the highest probability of providing the largest contribution for the shear strengthening of the RC beam, four strain gauges (SG_L) were bonded in each laminate as shown in Fig. 4. Adopting the same principle, one steel stirrup was monitored with three strain gauges (SG_S) installed according to the configuration represented in Fig. 4. The location of the monitored laminates and stirrups in the tested beams is indicated in Fig. 2.

1 **3. EXPERIMENTAL RESULTS AND DISCUSSION**

2 **3.1 Load carrying capacity of the tested beams**

3   The relationship between the applied force (F) and the deflection at the loaded section (u_{LS}) of the tested beams is

4 illustrated in Fig. 5a. In this figure, ΔF represents the increase of the load provided by the shear strengthening system,

5 while F^{3S-R} is the load capacity of the reference beam. The $\Delta F / F^{3S-R}$ ratio was evaluated for deflections greater than

6 the one corresponding to the formation of the first shear crack in the reference beam 3S-R, and the $\Delta F / F^{3S-R}$ *vs.* u_{LS}

7 relationship is illustrated in Fig. 5b. Assuming that $\Delta F_{max} = F_{max} - F_{max}^{3S-R}$, being F_{max}^{3S-R} and F_{max} the load carrying

8 capacity (maximum force) of the reference beam and of the NSM CFRP shear strengthened beam, respectively, the

9 $\Delta F_{max} / F_{max}^{3S-R}$ ratio was also evaluated. The values for F_{max}, $\Delta F_{max} / F_{max}^{3S-R}$ and the deflection at loaded section

10 corresponding to F_{max} ($u_{F_{max}}$) are presented in Table 3.

11   Fig. 5 and the results included in Table 3 show that, for deflections higher than the one corresponding to the

12 formation of the first shear crack in the reference beam, the adopted CFRP configurations provided an increase in the

13 beam's load carrying capacity. This reveals that the CFRP laminates bridging the surfaces of the shear crack offer

14 resistance, mainly to crack opening, resulting to a smaller degradation of the shear stress transfer between the faces of

15 the crack, due to aggregate interlock effect. Therefore, for deflections above the one corresponding to the formation of

16 the shear crack in the reference beam, an increase of the beam's stiffness was observed in the shear strengthened beams.

17 The crack opening resisting mechanisms provided by the laminates bridging the shear crack also contributed to increase

18 the load at which stirrups enter in their plastic phase.

19   The CFRP shear strengthening configurations provided an increase in terms of stiffness (after shear crack formation)

20 and maximum load (F_{max}). It is verified that $\Delta F_{max} / F_{max}^{3S-R}$ of the tested NSM CFRP shear strengthened beams has

21 varied between 21.2% and 82.6%. Regardless the percentage of the CFRP laminates, the strengthening arrangements

22 with vertical laminates had the small values of the increase in terms of beam's load carrying capacity ($\Delta F_{max} / F_{max}^{3S-R}$):

23 21.2% and 42.5% for the beams with four (3S-4LV beam with ρ_f = 0.044%) and seven (3S-7LV beam with ρ_f =

24 0.089%) vertical laminates, respectively. The value of $\Delta F_{max} / F_{max}^{3S-R}$ for the beams 3S-4LI (ρ_f = 0.056%) and 3S-9LI

25 (ρ_f = 0.113%), both with laminates inclined at 52º, was 48.4% and 82.6%, respectively. The best performance of the

26 shear strengthening solutions with inclined laminates is justified by the orientation of the shear failure cracks that had a

27 tendency to be almost orthogonal to the inclined laminates. Furthermore, for vertical laminates the total resisting bond

28 length of the CFRP was lower than that of inclined laminates. After the formation of a shear crack in the reference

1 beam, the $\Delta F_{max}\big/F_{max}^{3S-R}$ values of the strengthened beams with the larger percentage of CFRP (ρ_f) were higher than

2 the corresponding values of the beams strengthened with the lower ρ_f.

3   The deflection at the loaded section in correspondence to F_{max} ($u_{F_{max}}$) in all the NSM CFRP shear strengthened

4 beams was similar or larger than the value of $u_{F_{max}}$ obtained in the reference beam 3S-R (10.68 mm). The strengthening

5 arrangements with vertical laminates had the small values of $u_{F_{max}}$: 11.78 mm and 10.58 mm for the beams 3S-4LV

6 and 3S-7LV, respectively. The value of $u_{F_{max}}$ for the beams 3S-4LI and 3S-9LI, both with laminates inclined at 52º,

7 was 13.35 mm and 18.21 mm, respectively.

8

9 **3.2 Failure modes**

10   As expected, all the tested beams failed in shear in the shear span a. Fig. 6 shows the crack patterns at failure of the

11 tested beams in the shear span a. The maximum load of the reference beam (3S-R) was attained when one stirrup

12 crossing the shear failure crack has ruptured. In the NSM CFRP shear strengthened beams no laminate has ruptured up

13 to peak load.

14   In the 3S-4LV beam, at a load level of about 363 kN the second laminate from the loaded section debonded at its top

15 part (laminate 2 in Fig. 6b), with a formation of a concrete volume surrounding the laminate. This was followed by a

16 decay of the load carrying capacity of this beam (Fig. 5a). The load was transferred, mainly, to the third laminate from

17 the loaded section (laminate 3 in Fig. 6b), and the load was again increased up to the moment (F_{max} = 401.8 kN) when

18 occurred the debonding of the bottom part of this laminate, followed by a sudden and abrupt load decay. The maximum

19 load of the beam 3S-7LV (F_{max} = 472.1 kN) was attained immediately before the debonding of the bottom part of the

20 laminate 4 (Fig. 6c). After the maximum load, it was verified the debonding of the top part of laminate 3 (Fig. 6c).

21   In the 3S-4LI beam, at a load level of about 462 kN the 4th laminate from the loaded section debonded at its bottom

22 part (laminate 4 in Fig. 6d), with a formation of a concrete volume surrounding the laminate. This was followed by a

23 decay of the load carrying capacity of this beam (Fig. 5a). The load was transferred, mainly, to the second and third

24 laminates from the loaded section (laminates 2 and 3 in Fig. 6d), the ones crossing the critical shear crack, and the load

25 was again increased up to the moment (F_{max} = 491.7 kN) when occurred the debonding of the top part of the laminate

26 2, followed by a sudden and abrupt load decay. In the 3S-9LI beam, at a load level of about 562 kN the third laminate

27 from the loaded section debonded at its top part (laminate 3 in Fig. 6e), with a formation of a concrete volume

28 surrounding the laminate. This was followed by a decay of the load carrying capacity of this beam (Fig. 5a). The load

29 was transferred, mainly, to the 4th laminate from the loaded section (laminate 4 in Fig. 6e), and the load was again

increased up to the moment (F_{max} = 605 kN) when occurred the debonding of the top part of this laminate (Fig. 6e), followed by a sudden and abrupt load decay.

3.3 Strains in the CFRP laminates and steel stirrups

Table 4 includes the strains measured in the monitored laminates at F_{max}, $\varepsilon_{CFRP}^{SG-Li}$ (i=1 to 4, see Fig. 4), and the maximum strain in these laminates up to F_{max}, ε_{CFRP}^{max}, for the tested NSM CFRP shear strengthened beams. The strains were dependent on the relative distance between the strain gauges (SG) and the shear failure crack crossing the laminate. It was verified that the ε_{CFRP}^{max} has varied between 9.6‰ and 14.4‰. These values ranged between 54% and 81% of the ultimate tensile strain of the adopted CFRP laminates (ε_{fu}=17.8‰) justifying the high strengthening effectiveness provided by NSM CFRP laminates for the shear strengthening of relatively high T cross section RC beams. Comparing the ε_{CFRP}^{max} in the laminates at different orientations, a clear tendency for lower values of the strains in vertical laminates is observable.

Fig. 7 illustrates the variation of the strains on the monitored laminates during the loading process of the beam up to its maximum load. It is observed that the curves featured two phases. In the initial stage of loading, while the CFRP was not crossed by a diagonal crack, the contribution of the laminate for the beam's load-carrying capacity was marginal. The second stage initiates when the CFRP was crossed by a diagonal crack. The gradient of the strains registered in the SGs was the higher the closer was the SG from the critical shear crack. This behavior was similar in the monitored stirrups (Fig. 8). The evolution of the strains in the steel stirrups indicates that when the strengthened beams failed, the steel stirrups had already developed a significant plastic deformation.

3.4 Comparison of the shear strengthening effectiveness

The shear capacity contributed by the CFRP (V_f) was obtained by subtracting the shear resistance of the reference beam ($V_{ref.}$) from the shear resistance of the strengthened beam (V_t):

$$V_t = V_{ref.} + V_f \qquad (1)$$

In this approach it is assumed that the steel stirrups give the same contribution in the strengthened and in the corresponding reference beam.

By comparing the V_f values of the beams of the present experimental program (46.9 kN, 93.8 kN, 106.9 kN and 182.4 kN for the beams 3S-4LV, 3S-7LV, 3S-4LI and 3S-9LI, respectively) to those determined in NSM shear strengthened RC beams [11] with the same kind of concrete (f_{cm} = 39.7 MPa) and the same test setup, but with RC

1 beams of smaller height of the cross section, 400 mm, (Fig. 9a), it can be concluded that the effectiveness of the NSM

2 technique with CFRP laminates increases with the height of the cross section.

3   From the V_f values, the effective strain in the laminates, ε_{fe}, for the tested beams can be obtained from the following

4 equation [11]:

$$\varepsilon_{fe} = V_f \Big/ \left(h_w \times \frac{A_{fv}}{s_f} \times E_f \times \left(\cot g\ \alpha + \cot g\ \theta_f \right) \times \sin \theta_f \right) \tag{2}$$

5 where h_w is the height of the beam's web, A_{fv} is the cross sectional area of a "laminate stirrup" that is formed by two

6 lateral laminates ($A_{fv} = 2 \times a_f \times b_f$), s_f is the spacing of laminates, E_f is the elastic modulus of the laminate, α is the

7 orientation of the shear failure crack (considered as 45°), and θ_f is the inclination of the laminates with respect to the

8 beam axis (Fig. 10).

9   Fig. 9b compares the ε_{fe} values obtained in the present experimental program (6.9‰ for the beams with vertical

10 laminates; 11.3‰ and 9.6‰ for the beams 3S-4LI and 3S-9LI, respectively) with those obtained in Dias and Barros

11 [11] with the same kind of concrete (f_{cm} = 39.7 MPa) and the same test setup, where the height of the cross section was

12 400 mm. In Fig. 9b is again visible that the effectiveness of the NSM technique with CFRP laminates increases with the

13 height of the cross section.

14

15 **4. APPRAISAL OF THE PREDICTIVE PERFORMANCE OF ANALYTICAL FORMULATIONS**

16   Taking the results obtained in the tested beams shear strengthened using NSM technique with CFRP laminates, the

17 performance of the analytical formulations proposed by Nanni *et al.* [13] and Dias and Barros [11] for the prediction of

18 the contribution of NSM CFRP systems for the shear resistance of RC beams was appraised.

19

20 **4.1 Formulation by Nanni *et al.* [13]**

21   According to the formulation proposed by Nanni *et al.* [13], the term within the square brackets of the equation (3)

22 is the force resulting from the tensile stress in the NSM FRP elements crossing the shear failure crack. The vertical

23 projection of this force is the contribution of the FRP to the shear resistance of the beam (V_f),

$$V_f = \left[4 \cdot \left(a_f + b_f \right) \cdot \tau_b \cdot L_{tot\,min} \right] \cdot \sin \theta_f \tag{3}$$

24 being τ_b the average bond stress of the FRP elements intercepted by the shear failure crack, and $L_{tot\,min}$ is obtained

25 from (see Fig. 11),

$$L_{tot\,min} = \sum_i L_i \tag{4}$$

1 where L_i represents the length of each single NSM laminate crossed by a 45-degree shear crack, determined from,

$$L_i = \begin{cases} min\left(\dfrac{s_f}{cos\,\theta_f + sin\,\theta_f}\, i;\; l_{max} \right) & i = 1.....\dfrac{N}{2} \\ \\ min\left(l_{net} - \dfrac{s_f}{cos\,\theta_f + sin\,\theta_f}\, i;\; l_{max} \right) & i = \dfrac{N}{2}+1.....N \end{cases} \tag{5}$$

2 $L_{tot\;min}$ corresponds to an arrangement of the FRP reinforcements crossing the shear failure crack that leads to the

3 minimum of the $\sum\limits_i L_i$. In (5) l_{net} is defined as,

$$l_{net} = l_b - \frac{2c}{sin\,\theta_f} \tag{6}$$

4 which represents the net length of a FRP laminate, as shown in Fig. 11, to account for cracking of the concrete cover

5 and installation tolerances. In (6), l_b is the actual length of a FRP laminate and c is the concrete clear cover thickness.

6 The first limitation of (5) takes into account bond as the controlling failure mechanism, and represents the minimum

7 effective length of a FRP laminate intercepted by a shear crack as a function of the term N,

$$N = \frac{l_{eff}\left(1 + cot\,\theta_f\right)}{s_f} \tag{7}$$

8 where N is rounded off to the lowest integer (e.g., $N=5.7 \Rightarrow N = 5$), and l_{eff} represents the length of the vertical

9 projection of l_{net} as shown in Fig. 11,

$$l_{eff} = l_b\,sin\,\theta_f - 2c \tag{8}$$

10 The second limitation in (5), $L_i = l_{max}$, results from the force equilibrium condition, taking an upper bound value for

11 the effective strain, ε_{fe} (see Fig. 12),

$$l_{max} = \frac{\varepsilon_{fe}}{2} \cdot \frac{a_f \cdot b_f}{a_f + b_f} \cdot \frac{E_f}{\tau_b} \tag{9}$$

12 Considering for ε_{fe} and τ_b the values recommended by Barros and Dias [7], respectively, 0.59% and 16.1 MPa,

13 and assuming for the elastic modulus of the laminate the average value recorded in the experimental program of the

14 present work (169.2 GPa), the values of the contribution of the NSM laminates for the shear strengthening of the tested

15 beams (V_f^{Ana}), included in Table 5, were compared to those registered experimentally (V_f^{Exp}). The values of the

16 $V_f^{Exp.}/V_f^{Ana}$ ratio ranged between 1.68 and 2.42, and an average value of about 1.96 for $V_f^{Exp.}/V_f^{Ana}$ was obtained (the

17 coefficient of variation was 18%). These values show that the formulation proposed by Nanni $et\;al.$ [13] is very

18 conservative when the NSM CFRP laminates are installed into the slits of relatively high T cross section RC beams.

10

4.2 Formulation by Dias and Barros [11]

According to the formulation proposed by Dias and Barros [11], the contribution of the NSM CFRP laminates for the shear capacity of a RC beam, identified by V_f, can be obtained using the equation (10):

$$V_f = h_w \times \frac{A_{fv}}{s_f} \times \varepsilon_{fe} \times E_f \times \left(cotg\ \alpha + cotg\ \theta_f \right) \times sin\theta_f \qquad (10)$$

The value of the effective strain in the laminates (ε_{fe}) is obtained from:

$$\varepsilon_{fe} = \left[3.76888 \times e^{\left(-0.1160261\theta_f + 0.0010437\theta_f^2 \right)} \times \left[\left(E_f\rho_f + E_s\rho_{sw} \right) / \left(f_{cm}^{2/3} \right) \right]^{-0.460679 \times e^{\left(0.0351199\theta_f - 0.0003431\theta_f^2 \right)}} \right] / \gamma_f \qquad (11)$$

In equation (11), ρ_f and ρ_{sw} are introduced like a ratio and not in percentage (values obtained with the equations in the footnote of Table 1, but eliminating the term 100), f_{cm} is the average concrete compressive strength in cylinders (in MPa), E_s is the elasticity modulus of the steel stirrups (in MPa, the same units should be use for the elasticity modulus of the laminate E_f) and γ_f is an uncertainty factor equal 1.3. The meaning of the others parameters of equations (10) and (11) was described in the section 3.4 (see also Fig. 10).

Adopting the formulation proposed by Dias and Barros [11], the obtained values of the contribution of the NSM laminates for the shear strengthening of the tested beams (V_f^{Ana}) are included in Table 5 and were compared to those registered experimentally (V_f^{Exp}). The values of the $V_f^{Exp.}/V_f^{Ana}$ ratio ranged between 1.37 and 1.63, and an average value of about 1.51 for $V_f^{Exp.}/V_f^{Ana}$ was obtained (the coefficient of variation was 7%).

Considering the results of the Table 5 and Figure 13 it can be concluded that for relatively high T cross section RC beams the formulation proposed by Dias and Barros [11] provided more realistic predictions for the shear capacity contributed by the CFRP (V_f). For the better performance of the formulation of Dias and Barros [11], it contributed the fact that this formulation considers parameters that are related to the performance of RC beams shear strengthened with NSM technique using CFRP laminates, whose evaluation was based on the obtained experimental results, namely: concrete strength, percentage of existing steel stirrups, percentage and orientation of the CFRP.

5. CONCLUSIONS

To appraise the possibility of the application of NSM CFRP laminates for the shear strengthening of relatively high T cross section RC beams having a certain percentage of existing steel stirrups, an experimental program was carried out. The height of the T cross section of the tested RC beams was 600 mm.

From the obtained experimental results, it can be concluded that NSM shear strengthening technique with CFRP laminates is very effective in RC beams of relatively high cross section, not only in terms of increasing the overall

11

behavior of the beams, but also in assuring higher mobilization of the tensile capacity of the CFRP. The NSM CFRP shear strengthening configurations provided an increase in terms of maximum load (F_{max}) that ranged between 21% (ρ_f=0.044%) and 83% (ρ_f=0.113%) of the maximum load of the reference beam. In general, the values of the deflection at the loaded section in correspondence to F_{max} of the strengthened beams were higher than those occurred in the reference beam. Inclined laminates were more effective than vertical laminates, and the shear resistance of the beams increased with the percentage of laminates. The maximum tensile strain recorded in the NSM CFRP laminates up to the maximum load ranged from 54% to 81% of its ultimate tensile strain, indicating that this strengthening technique can mobilize high stress levels in the CFRP. A very important aspect of the effectiveness of the NSM technique, regarding the analyzed beams, is its capacity to mobilize the yield stress of the stirrups before the maximum load of the strengthened beams has been attained.

Considering available experimental results obtained with the same test setup but using RC beams of lower T cross section (h = 400 mm instead of h = 600 mm), it was verified that the shear strengthening effectiveness of the NSM technique has increased with the height of the cross section.

In general, the formulation proposed by Dias and Barros [11] provided safe and acceptable estimates for the contribution of the NSM shear strengthening systems (the predicted values of the CFRP contribution for the shear resistance were 67% of the results registered experimentally). The formulation proposed by Nanni *et al.* [13] provided very conservative predictions when the NSM CFRP laminates were applied on relatively high T cross section RC beams (the predicted values of the CFRP contribution for the shear resistance were 51% of the results registered experimentally). Furthermore, the scatter of the results in terms of the $V_f^{Exp.}/V_{fd}^{Ana}$ ratio for the Dias and Barros [11] formulation was also quite low (the coefficient of variation was 7% and 18% for the formulations provided by Dias and Barros [11] and Nanni *et al.* [13], respectively).

REFERENCES

1. Bousselham A. and Chaallal O., "Shear strengthening reinforced concrete beams with fiber-reinforced polymer: assessment of influencing parameters and required research", ACI Structural Journal, 101(2), 219-227 (2004).

2. Mosallam, A. and Banerjee, S., "Shear enhancement of reinforced concrete beams strengthened with FRP composites laminates", Composites: Part B, 38, 781-793 (2007).

3. Kim, G., Sim, J. and Oh, H., "Shear strength of strengthened RC beams with FRPs in shear", Construction and Building Materials, 22(6), 1261-1270 (2008).

4. Mofidi, A. and Chaallal, O., "Shear strengthening of RC beams with externally bonded FRP composites: Effect of strip-width-to-strip-spacing ratio", Journal of composites for construction, 15(5), 732-742 (2011).

5. De Lorenzis, L. and Nanni, A., "Shear Strengthening of Reinforced Concrete Beams with Near-Surface Mounted Fiber-Reinforced Polymer Rods", ACI Structural Journal, 98(1), 60-68 (2001).

6. Carolin, A., "Carbon fibre reinforced polymers for strengthening of structural elements", PhD thesis, Lulea University of Technology (2003).

7. Barros, J.A.O. and Dias, S.J.E., "Near surface mounted CFRP laminates for shear strengthening of concrete beams", Journal Cement and Concrete Composites, 28(3), 276-292 (2006).

8. El-Maaddawy, T., "Restoration of Concrete Beams Presubjected to Cycles of Shear Damage", ACI Structural Journal, 112(3), 347-358 (2015).

9. El-Hacha, R. and Riskalla, S.H., "Near-surface-mounted fiber-reinforced polymer reinforcements for flexural strengthening of concrete structures", ACI Structural Journal, 101(5), 717-726 (2004).

10. Dias, S.J.E., and Barros J.A.O., "Performance of reinforced concrete T beams strengthened in shear with NSM CFRP laminates", Engineering Structures, 32(2), 373-384 (2010).

11. Dias, S.J.E., and Barros, J.A.O., "Shear strengthening of RC beams with NSM CFRP laminates: experimental research and analytical formulation", Composite Structures, 99, 477-490 (2013).

12. Bianco, V., Barros, J.A.O., and Monti, G., "Bond model of NSM-FRP in the context of the shear strengthening of RC beams," ASCE Structural Engineering Journal, 135(6), 619-631 (2009).

13. Nanni, A., Di Ludovico, M. and Parretti, R., "Shear strengthening of a PC bridge girder with NSM CFRP rectangular bars", Advances in Structural Engineering, 7(4), 97-109 (2004).

14. Collins, M. P., and Mitchell, D., "Prestressed Concrete Structures", Prentice-Hall, Inc., Englewood Cliffs, New Jersey (1997).

15. EN 206-1, "Concrete - Part 1: Specification, performance, production and conformity," European standard, CEN, 69 pp., 2000.

16. EN 10002-1, "Metallic materials - Tensile testing. Part 1: Method of test (at ambient temperature)", European Standard, CEN, Brussels, Belgium, 35 pp., 1990.

17. ISO 527-5, "Plastics - Determination of tensile properties - Part 5: Test conditions for unidirectional fiber-reinforced plastic composites", International Organization for Standardization (ISO), Geneva, Switzerland, 9 pp., 1997.

18. Costa, I.G.; and Barros, J.A.O., "Tensile creep of a structural epoxy adhesive: experimental and analytical characterization", International Journal of Adhesion & Adhesives, 59, 115-124 (2015).

19. ISO 527-2, "Plastics - Determination of tensile properties - Part 2: Test conditions for moulding and extrusion plastics" International Organization for Standardization, 1993.

1 **List of Tables:**

2 Table 1 - General information about the series of the tested RC beams.

3 Table 2 - Average values of the properties of the steel.

4 Table 3 - Experimental results of the tested RC beams.

5 Table 4 - Strain values in the CFRP laminates.

6 Table 5 - Experimental *vs.* analytical results.

1   **List of Figures:**

2   **Fig. 1** - Geometry of the reference beam, steel reinforcements common to all of the tested beams, support and load

3   conditions (dimensions in mm).

4   **Fig. 2** - NSM CFRP shear strengthening configurations (laminates at dashed lines) and localization of the monitored

5   laminates and steel stirrups in the tested beams (dimensions in mm).

6   **Fig. 3** - a) and b) NSM CFRP laminates shear strengthening technique; c) test setup.

7   **Fig. 4** - Position of the strain gauges in the monitored CFRP laminates and in the monitored steel stirrups (dimensions

8   in mm).

9   **Fig. 5** - a) Force *vs.* deflection at loaded section of the tested beams and b) $\Delta F/F^{3S\text{-}R}$ *vs.* deflection at loaded section of

10   the NSM CFRP tested beams..

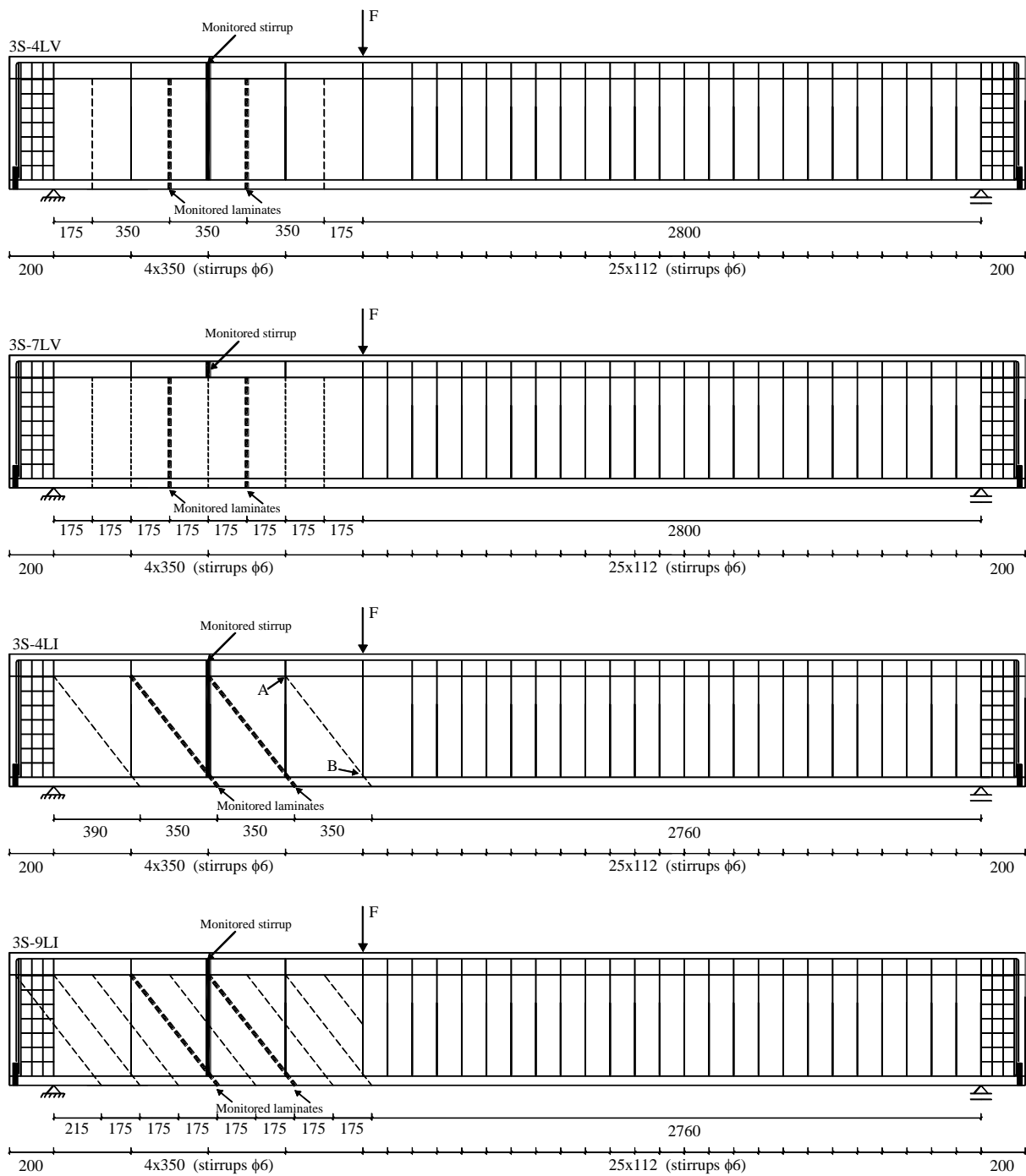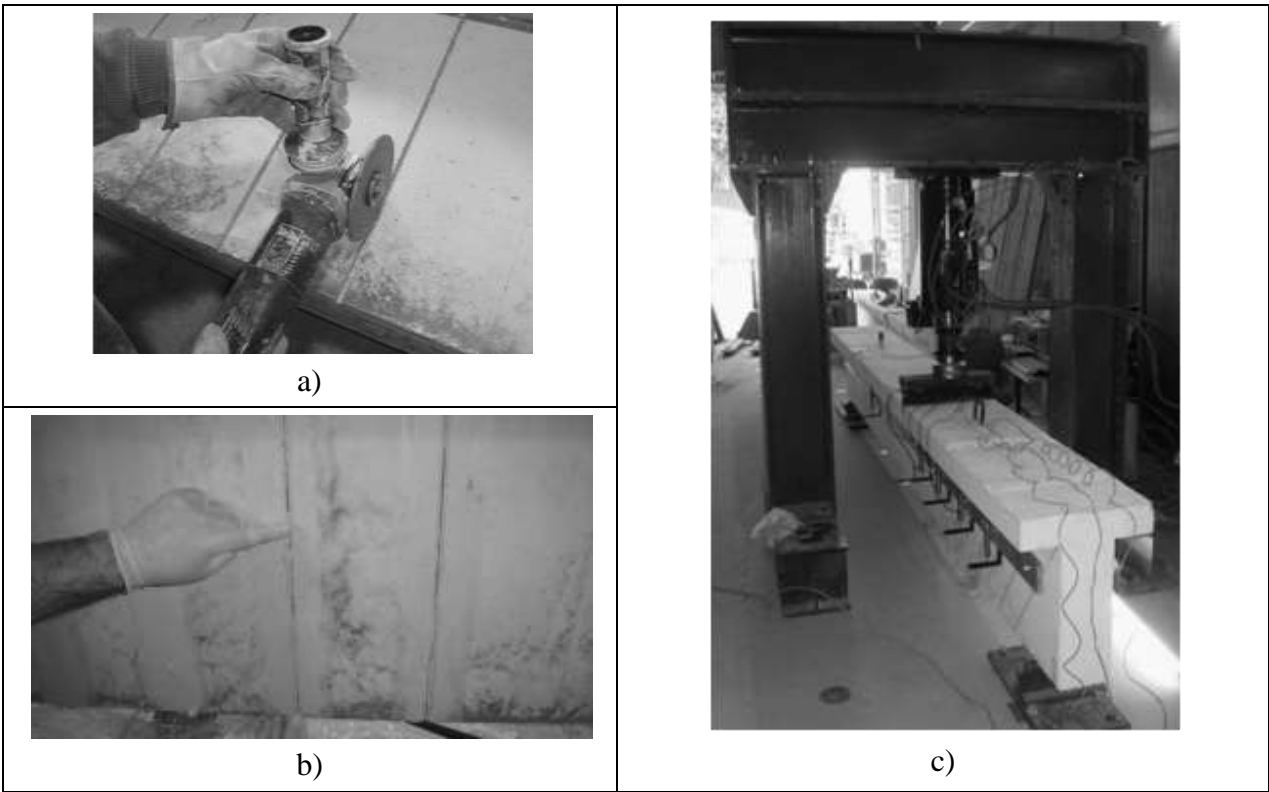11   **Fig. 6** - Crack patterns of the tested beams at failure.

12   **Fig. 7** - Variation of strains in the monitored CFRP laminates of the tested beams.

13   **Fig. 8** - Variation of strains in the monitored steel stirrups of the tested beams.

14   **Fig. 9** - Comparison of the shear strengthening effectiveness of the NSM technique with CFRP laminates in terms of: a)

15   V_f and b) ε_{fe}.

16   **Fig. 10** - Data for the analytical definition of the effective strain of the CFRP used in the formulation proposed by Dias

17   and Barros.

18   **Fig. 11** - Graphical representation of variables used in the formulation proposed by Nanni *et al.* (for this example

19   $\sum_{i} L_i = L_2 + L_3 + L_4$).

20   **Fig. 12** - Graphical representation of l_{max}.

21   **Fig. 13** - a) Comparison between the experimental and analytical values of the NSM CFRP contribution for the shear

22   resistance, V_f, and b) ($V_{f,\ Exp}\ /\ V_{f,\ Ana}$) *vs.* percentage of CFRP (ρ_f). [Note: VL - vertical laminates; IL - inclined

23   laminates].

24

25

1   Table 1 - General information about the series of the tested RC beams.

Beam	ρ_{sl} (%) [1]	ρ_{sw} (%) [2]	a/d	NSM CFRP laminates	θ_f (°)	s_f (mm)	ρ_f (%) [3]
3S-R				-	-	-	-
3S-4LV				2×4	90	350	0.044
3S-7LV	2.0	0.09	2.5	2×7	90	175	0.089
3S-4LI				2×4	52	350	0.056
3S-9LI				2×9	52	175	0.113

2 (1) The percentage of the longitudinal tensile reinforcement was obtained from $\rho_{sl} = (A_{sl}/(b_w \times d)) \times 100$, where A_{sl} is the cross sectional area
3 of the longitudinal tensile steel reinforcement (see Fig. 1), $b_w = 180$ mm is the width of the beam's web and d is the distance from extreme
4 compression fiber to the centroid of tensile reinforcement. (2) The percentage of the vertical steel stirrups was obtained from
5 $\rho_{sw} = (A_{sw}/(b_w \times s_w)) \times 100$, where A_{sw} is the cross sectional of the two vertical arms of a steel stirrup, and s_w is the spacing of the stirrups. (3)
6 The CFRP percentage was obtained from $\rho_f = ((2 \times a_f \times b_f)/(b_w \times s_f \times sin\theta_f)) \times 100$, where a_f and b_f are the dimensions of the laminate
7 cross section, and s_f is the CFRP spacing.

8
9
10
11
12
13
14   Table 2 - Average values of the properties of the steel.

Diameter (mm)	ϕ6	ϕ12	ϕ16	ϕ32
Yield stress [f_{sym}] (MPa)	555	562	560	734
Tensile strength [f_{sum}] (MPa)	683	662	675	885

Table 3 - Experimental results of the tested RC beams.

Beam	F_{max} (kN)	$\Delta F_{max} / F_{max}^{3S-R}$ (%)	F_{max} / F_{max}^{3S-R}	$u_{F_{max}}$ (mm)
3S-R	331.4	0	1.00	10.68
3S-4LV	401.8	21.2	1.21	11.78
3S-7LV	472.1	42.5	1.42	10.58
3S-4LI	491.7	48.4	1.48	13.35
3S-9LI	605.0	82.6	1.83	18.21

Table 4 - Strain values in the CFRP laminates.

Beam	Monitored laminate[1]	$\varepsilon_{CFRP}^{SG\_L1}$ (‰)	$\varepsilon_{CFRP}^{SG\_L2}$ (‰)	$\varepsilon_{CFRP}^{SG\_L3}$ (‰)	$\varepsilon_{CFRP}^{SG\_L4}$ (‰)	ε_{CFRP}^{max} (‰)
3S-4LV	2	2.96 (7.64)	2.50	9.84	4.34	12.47
	3	0.54	11.60	12.47	11.33 (11.58)	
3S-7LV	3	4.79	9.57	0.95	2.00	9.57
	5	0.14 (0.15)	NA[2]	1.09 (5.56)	5.48 (5.52)	
3S-4LI	2	12.16	10.31	9.48	2.97 (3.28)	13.49
	3	NA[2]	8.41	13.49	5.64	
3S-9LI	4	13.84	10.82	14.39	7.90	14.39
	6	0.26 (0.29)	7.22	7.68 (8.08)	3.70 (5.92)	

(1) See Fig. 6. (2) This SG did not work. Note: The strain values in brackets are referred to the load when occurred the maximum strain in the laminates before the maximum load.

Table 5 - Experimental *vs.* analytical results.

Beam	Experimental	Analytical formulation			
		Nanni *et al.* [13]		Dias and Barros [11]	
	V_f^{Exp} (kN)	V_f^{Ana} (kN)	$V_f^{Exp.} / V_f^{Ana}$	V_f^{Ana} (kN)	$V_f^{Exp.} / V_f^{Ana}$
3S-4LV	46.9	28.0	1.68	34.2	1.37
3S-7LV	93.8	55.9	1.68	60.2	1.56
3S-4LI	106.9	44.1	2.42	72.5	1.47
3S-9LI	182.4	88.1	2.07	111.8	1.63
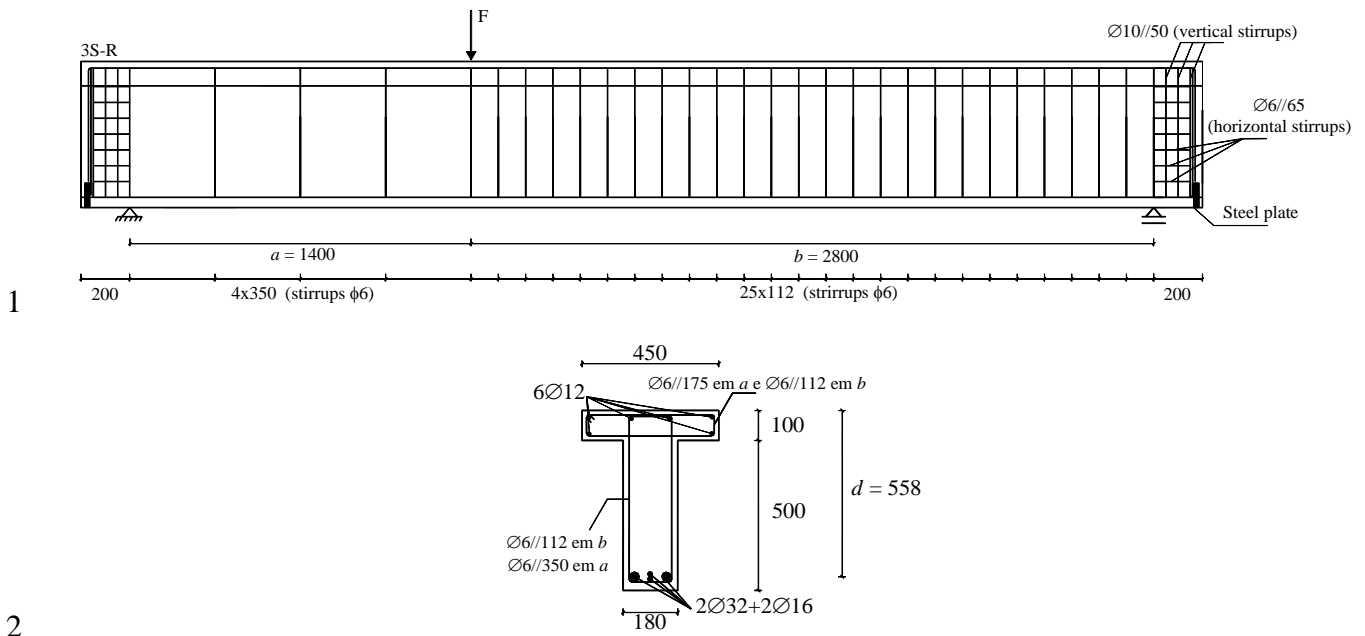
Fig. 1 - Geometry of the reference beam, steel reinforcements common to all of the tested beams, support and load conditions (dimensions in mm).

Fig. 2 - NSM CFRP shear strengthening configurations (laminates at dashed lines) and localization of the monitored laminates and steel stirrups in the tested beams (dimensions in mm).

Fig. 3 - a) and b) NSM CFRP laminates shear strengthening technique; c) test setup.
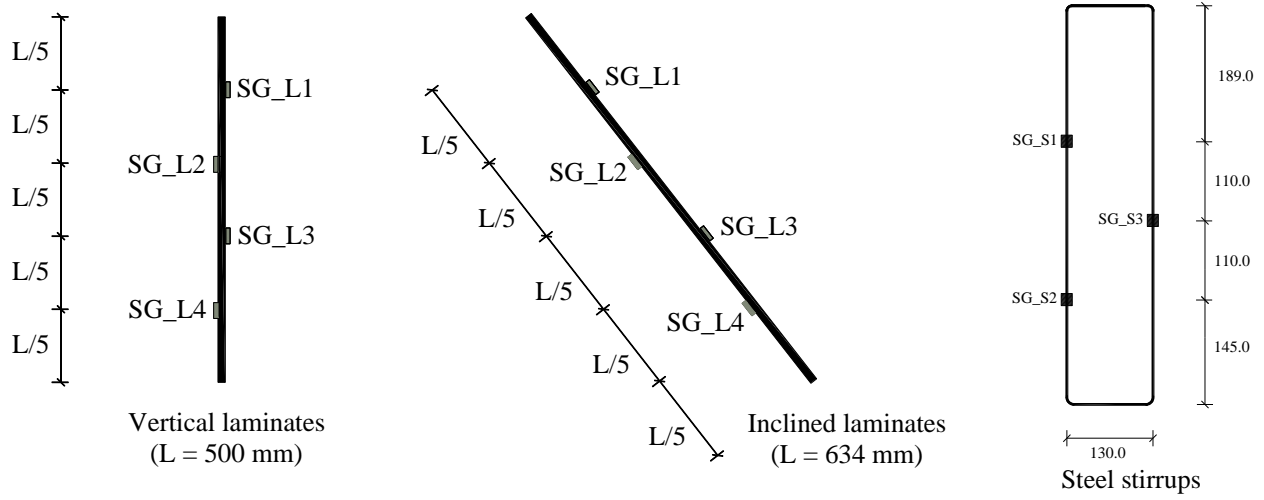
Vertical laminates
(L = 500 mm)

Inclined laminates
(L = 634 mm)

Steel stirrups

Fig. 4 - Position of the strain gauges in the monitored CFRP laminates and in the monitored steel stirrups (dimensions in mm).
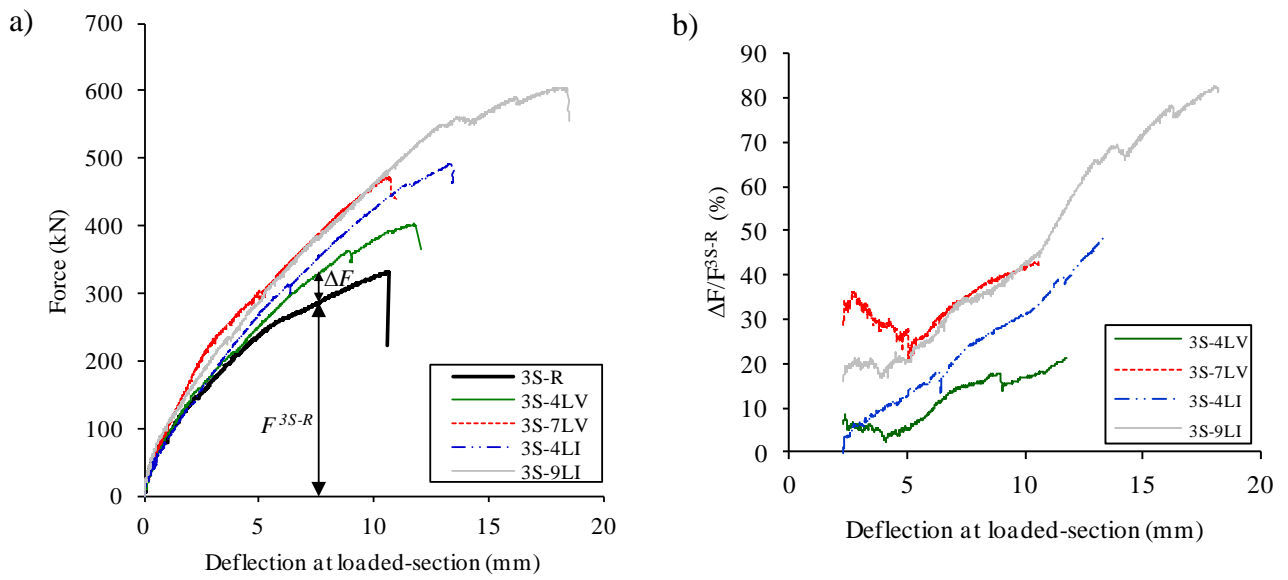
Fig. 5 - a) Force *vs.* deflection at loaded section of the tested beams and b) *ΔF/F^{3S-R} vs.* deflection at loaded section of the NSM CFRP tested beams.
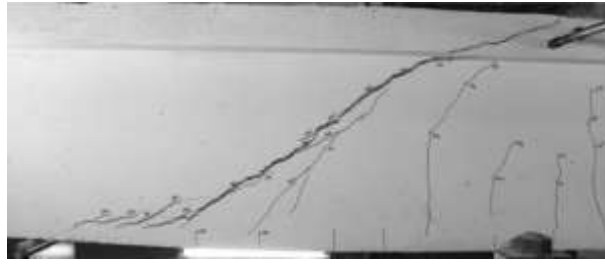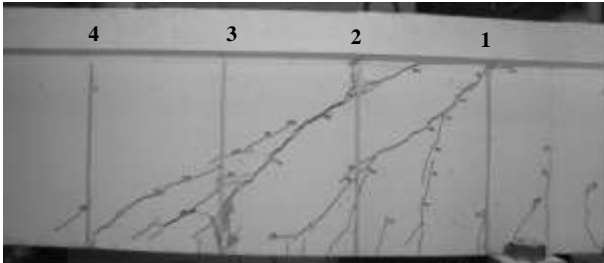
a) Beam 3S-R

b) Beam 3S-4LV

c) Beam 3S-7LV

d) Beam 3S-4LI

e) Beam 3S-9LI

Fig. 6 - Crack patterns of the tested beams at failure.

1
2
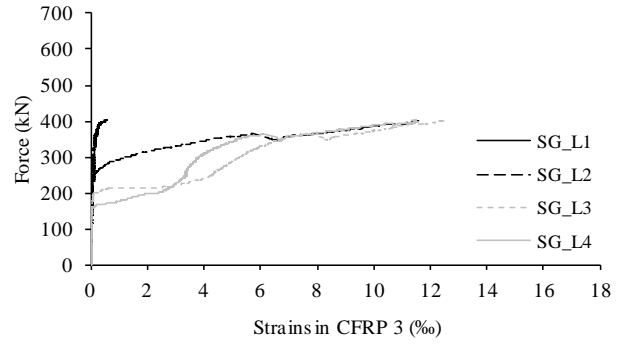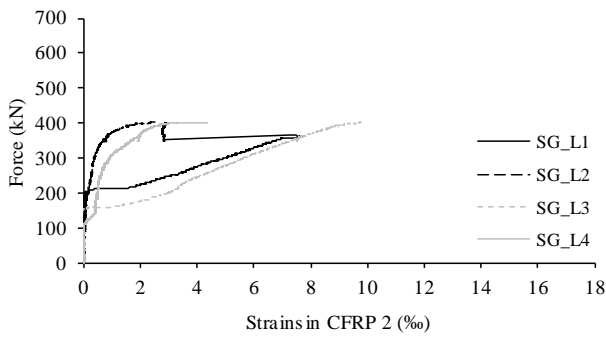
a) Beam 3S-4LV
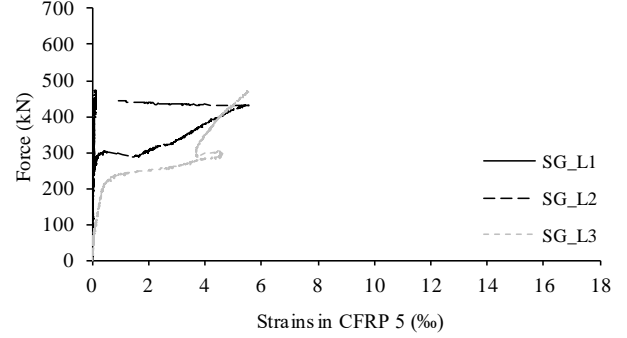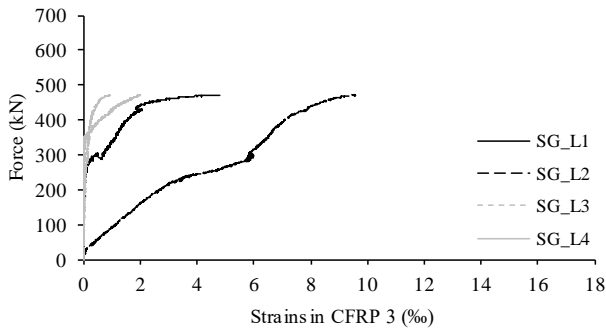
b) Beam 3S-7LV
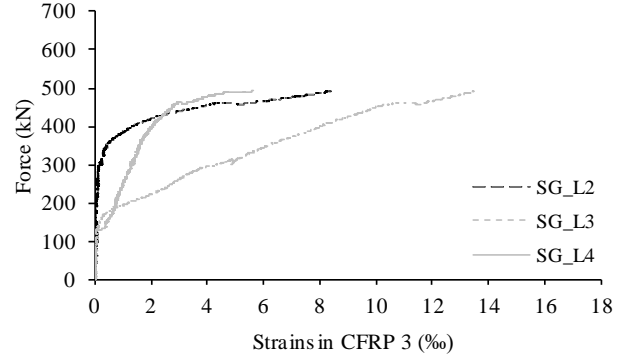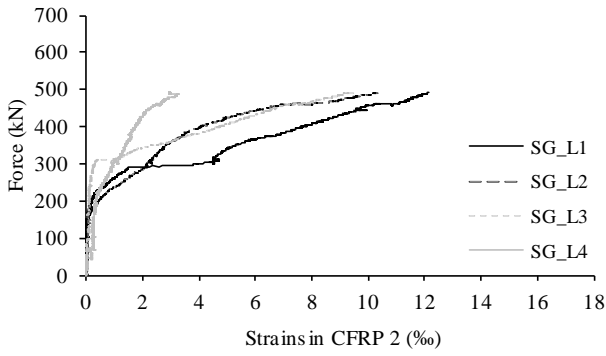
c) Beam 3S-4LI
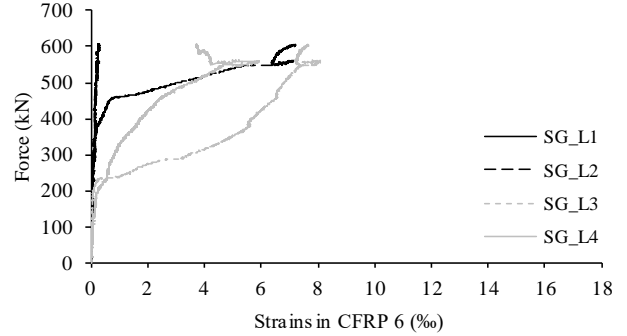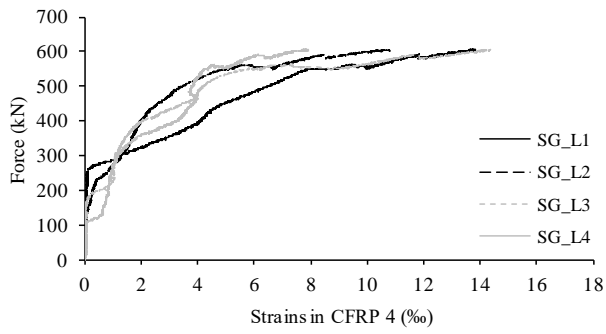
d) Beam 3S-9LI

1   Fig. 7 - Variation of strains in the monitored CFRP laminates of the tested beams.

2

25
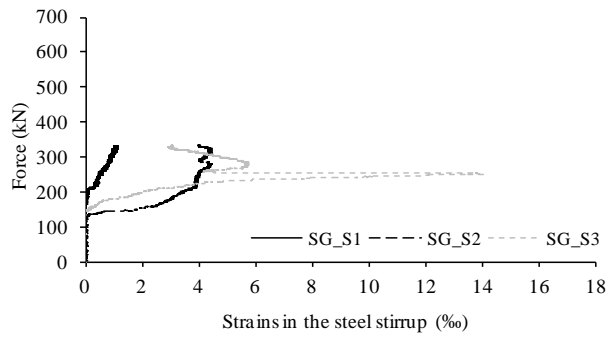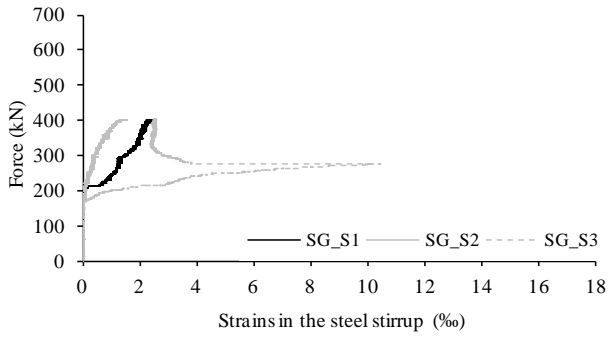
a) Beam 3S-R
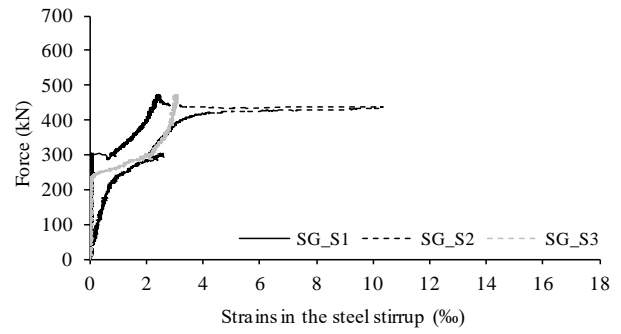
b) Beam 3S-4LV

c) Beam 3S-7LV
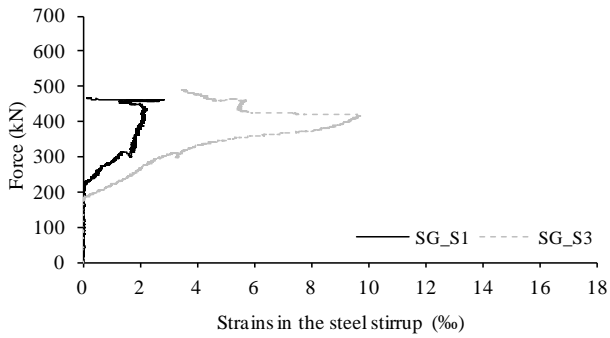
d) Beam 3S-4LI
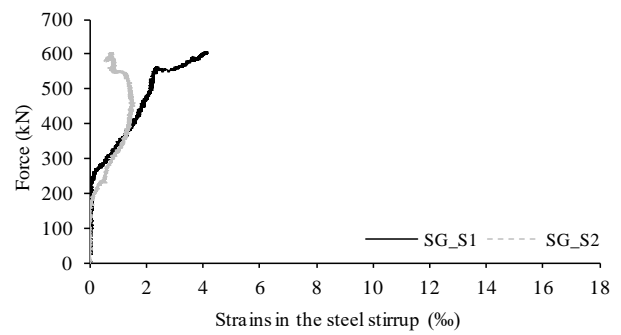
e) Beam 3S-9LI

Fig. 8 - Variation of strains in the monitored steel stirrups of the tested beams.

26

1

2   a)

3
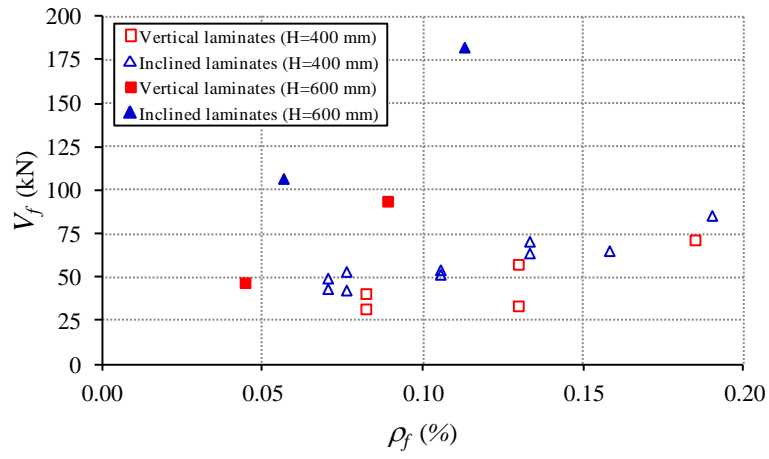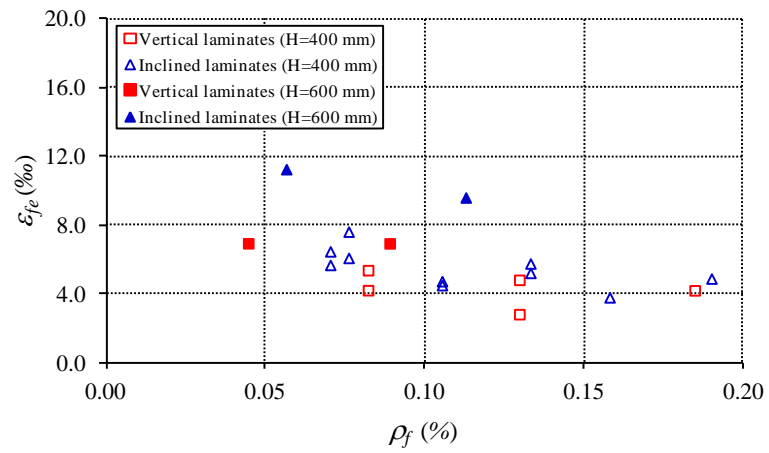
4   b)

Fig. 9 - Comparison of the shear strengthening effectiveness of the NSM technique with CFRP laminates in terms of: a)

V_f and b) ε_{fe}.

7
8
9
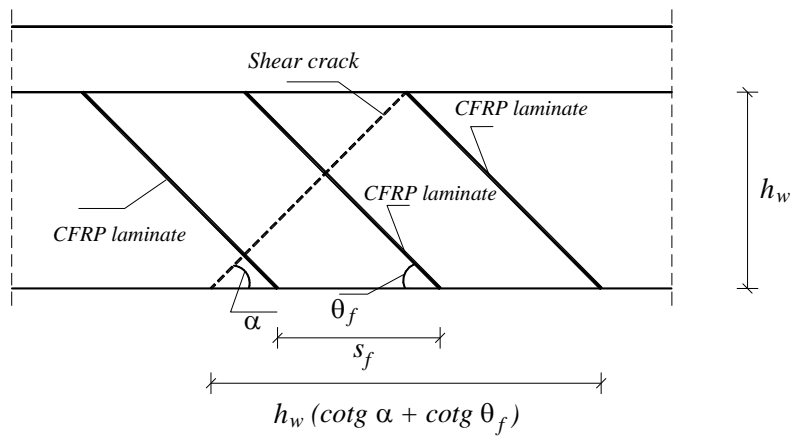
10
11   Fig. 10 - Geometric representation of the data for the analytical definition of the effective strain of the CFRP used in the
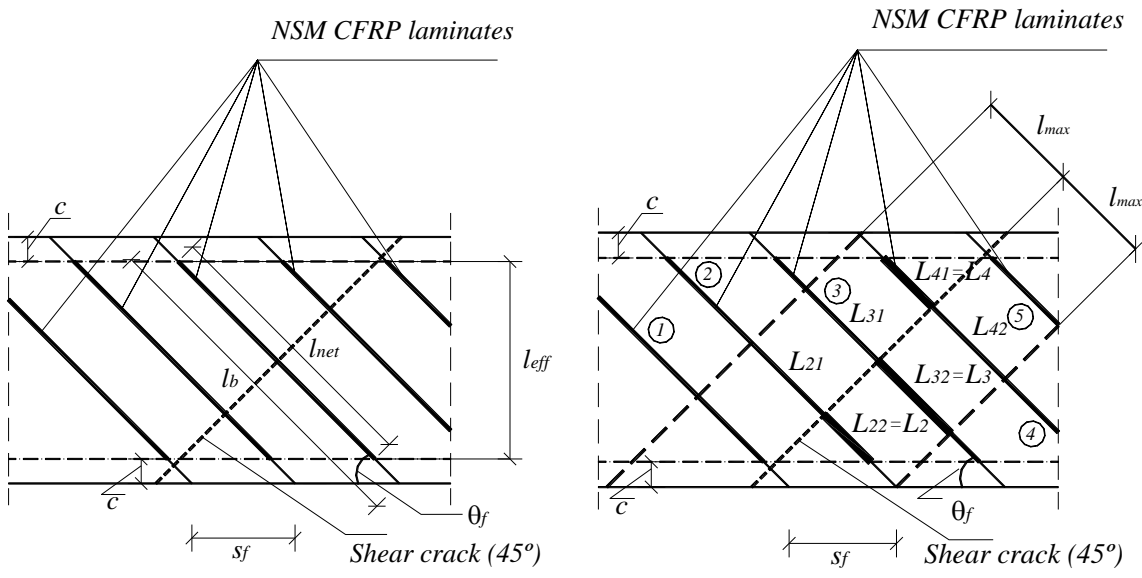12   formulation proposed by Dias and Barros.
13

Fig. 11 - Graphical representation of variables used in the formulation proposed by Nanni *et al.* (for this example $\sum_i L_i = L_2 + L_3 + L_4$).
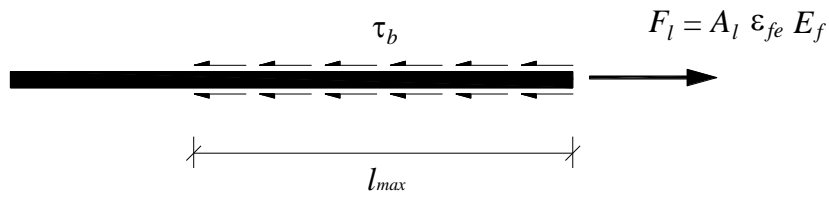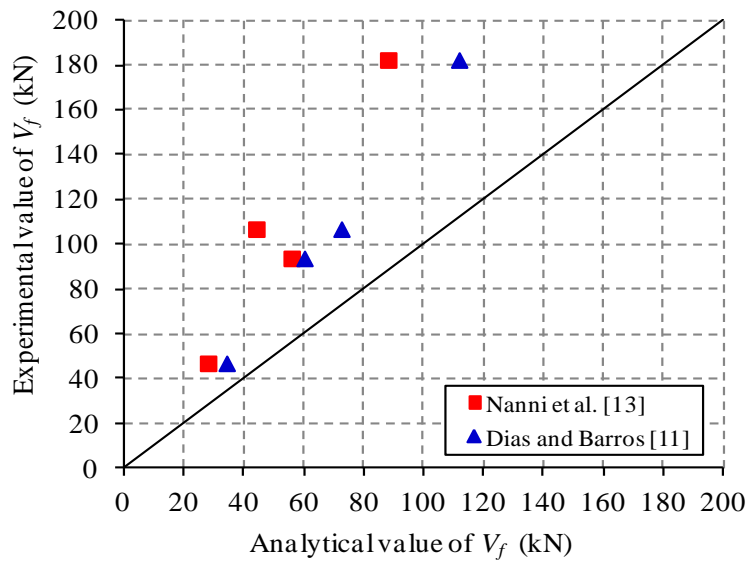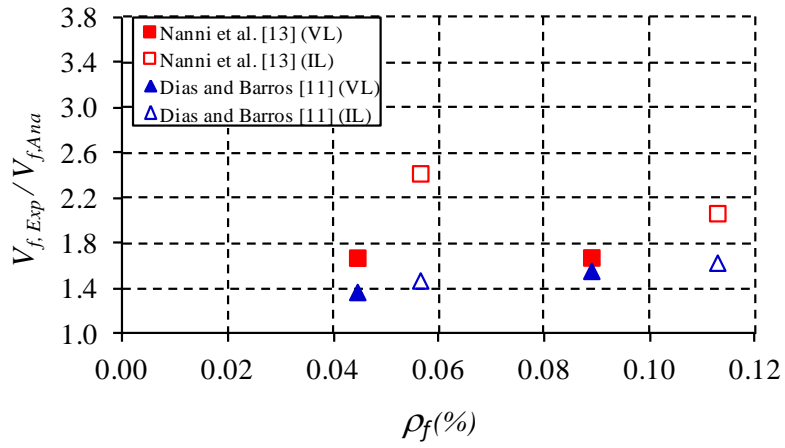

Fig. 12 - Graphical representation of l_{max}.

28

a)

b)

Fig. 13 - a) Comparison between the experimental and analytical values of the NSM CFRP contribution for the shear resistance, V_f, and b) ($V_{f, Exp} / V_{f, Ana}$) *vs.* percentage of CFRP (ρ_f). [Note: VL - vertical laminates; IL - inclined laminates].